

BENDING BEHAVIOUR OF COLD FORMED STEEL  
STRUCTURAL MEMBER WITH PERFORATED  
SECTION IN HOUSE FRAMING SYSTEM

LIM YON SHENG

SCHOOL OF CIVIL ENGINEERING  
UNIVERSITI SAINS MALAYSIA  
2017



**BENDING BEHAVIOUR OF COLD FORMED STEEL STRUCTURAL  
MEMBER WITH PERFORATED SECTION IN HOUSE FRAMING  
SYSTEM**

By

**LIM YON SHENG**

This dissertation is submitted to

**UNIVERSITI SAINS MALAYSIA**

As partial fulfilment of requirement for the degree of

**BACHELOR OF ENGINEERING (HONS.)  
(CIVIL ENGINEERING)**

School of Civil Engineering,  
Universiti Sains Malaysia

June 2017



**SCHOOL OF CIVIL ENGINEERING  
ACADEMIC SESSION 2016/2017**

**FINAL YEAR PROJECT EAA492/6  
FINAL DRAFT ENDORSEMENT FORM**

Title:

Name of Student:

I hereby declare that all corrections and comments made by the supervisor(s)  
And examiner have been taken into consideration and rectified accordingly.

Student's Signature:

Approved by:

\_\_\_\_\_

\_\_\_\_\_

(Signature of Supervisor)

Date:

Name of Supervisor :

Date :

Approved by:

\_\_\_\_\_

(Signature of Examiner)

Name of Examiner :

Date :



## **ACKNOWLEDGEMENT**

First and foremost, I would like to thank Universiti Sains Malaysia for giving me this opportunity to complete final year project dissertation. I would also like to thank my supervisor, Associate Professor Dr Fatimah De'nan. Throughout this final year, she has guided me and given me a lot of suggestions and guidance to produce a good quality project. Without her, I can hardly produce my result and complete my dissertation on time.

Next, my sincere and special thanks to Ling Jin Ying, who is year 2014-graduated student from USM for helping me in my nonlinear analysis study.

I would also like to thank my friends especially Lee Kenth Zheng and Zafira Nur Ezzati Bt Mustafa for supporting me and encouraging me to produce a better quality of dissertation.

## ABSTRACT

Due to highly demand of housing, the usage of cold formed steel section as framing system was introduced. C-channel cold-formed steel is widely used in construction industry due to its light weight, cost-effectiveness, and high strength-to-weight ratio. In order to reduce the weight of steel beams, accommodate plumbing and electrical facilities., web profile with openings has been introduced in the construction industry. In this study, bending behavior of cold-formed steel framing system and effective cost reduction between perforated and non-perforated steel section in steel framing system are investigated. The results are expressed in terms of displacement and yield moment. Using Staad.Pro and Lusas, a total of 26 set of nonlinear analyses were carried out to investigate the effects of opening spacing, edge distance and thickness of section on bending behavior. The result showed that increasing the opening spacing and edge distance would increase the bending capacity. C-channel steel section showed better moment resistance in thicker section. The result was then compared with the C-channel steel section without opening. From the analysis, it was observed that C-channel steel section without opening had higher bending capacity than C-channel steel section with opening in major axis. However, there is 0% of difference in terms of yield moment when comparing C-channel section with 0.4D of square opening and 0.3L edge opening as well as 0.1L opening space with C-channel section without opening while reducing the volumes up to 7.28%. Thus, C-channel section with 0.4D of square opening, 0.3L edge opening and 0.1L opening space give a very effective cost reduction.

## ABSTRAK

Keratan C terbentuk sejuk telah digunakan secara meluas dalam bidang aplikasi pembinaan. Senario ini berlaku disebabkan berat badannya yang ringan, kos efektif dan nisbah kekuatan kepada berat yang tinggi. Dalam usaha untuk menurunkan berat badan rasuk keluli, menampung kemudahan seperti paip dan wayar elektrik, bukaan pada web rasuk telah diperkenalkan dalam industri pembinaan. Dalam kajian ini, kesan lenturan pada keratan C terbentuk sejuk dan pengurangan kos efektif antara keratan C dengan bukaan dan tanpa bukaan dalam sistem rangka keluli rumah telah dianalisis. Keputusan analisis ditunjukkan daripada segi anjakan dan momen alah. Dengan menggunakan Staad.Pro dan Lusas, sebanyak 26 set analisis tidak linear telah dijalankan untuk menyelidik kesan dari segi jarak bukaan, jarak tepi, dan ketebalan keratan pada tingkah laku lenturan. Hasil kajian parametrik menunjukkan kekuatan lenturan menjadi semakin besar jikalau jarak bukaan dan jarak tepi ditambah. Keratan keluli C menunjukkan lenturan yang kuat dengan keratan yang lebih tebal. Keputusan dibandingkan dengan keratan C tanpa bukaan. Daripada analisis didapati bahawa keratan keluli C tanpa bukaan menunjukkan kekuatan lenturan yang lebih tinggi berbanding dengan keratan keluli C dengan bukaan pada paksi utama. Akan tetapi, tiada perbezaan dari segi momen alah apabila berbanding keratan C dengan bukaan berbentuk segi empat yang bersaiz  $0.4D$  dan  $0.3L$  jarak tepi serta  $0.1L$  jarak bukaan dengan keratan C tanpa bukaan di samping mengurangkan isipadu sehingga 7.28%. Oleh itu, keratan C dengan bukaan berbentuk segi empat yang bersaiz  $0.4D$  dan  $0.3L$  jarak tepi serta  $0.1L$  jarak bukaan memberikan pengurangan kos yang sangat efektif.



## TABLE OF CONTENT

ACKNOWLEDGEMENT .....	ii
ABSTRACT .....	iii
ABSTRAK .....	iv
TABLE OF CONTENT .....	v
LIST OF TABLE .....	viii
LIST OF FIGURE .....	ix
LIST OF SYMBOLS .....	xiii
Chapter 1 INTRODUCTION .....	1
1.1 Introduction .....	1
1.2 Cold-formed Steel (CFS).....	3
1.3 Characteristic of Cold-formed steel .....	3
1.3.1 Perforated Steel Section .....	5
1.4 Problem Statement.....	6
1.5 Objectives .....	6
1.6 Scope of Study .....	7
Chapter 2 LITERATURE REVIEW .....	8
2.1 Perforated Steel Section.....	8

2.2 Bending Resistance and Ultimate Strength.....	13
2.3 C-channel Cold Formed Steel Under Bending.....	14
2.4 Summary.....	14
Chapter 3 METHODOLOGY .....	15
3.1 Introduction .....	15
3.2 Numerical Study on Bending of C-channel Steel Section .....	15
3.2.1 Perforation Shapes and Sizes.....	16
3.2.2 Material Properties .....	16
3.2.3 Thickness of Section .....	16
3.2.4 Model Meshing.....	17
3.3 Finite Element Analysis LUSAS .....	18
3.3.1 LUSAS Procedure in Modelling Process .....	19
3.4 Convergence Study .....	37
3.5 Summary .....	39
Chapter 4 RESULTS AND DISCUSSION .....	40
4.1 Introduction .....	40
4.2 Variables .....	42
4.3 Determination of Moment Capacity of C-Channel Steel Section.....	43

4.4 Parametric Study .....	43
4.4.1 Effect of Spacing and Edge Distance of Opening .....	49
4.4.2 Effect of Thickness .....	56
4.5 Deformation Shapes .....	60
4.6 Summary .....	62
Chapter 5 CONCLUSION AND RECOMMENDATION .....	64
5.1 Conclusion .....	64
5.2 Recommendation for Future Research .....	65
REFERENCES .....	66
APPENDIXES	

## LIST OF TABLES

Table 1.1: Table 1.1 Increase of population in Malaysia from 2000 to 2017 (Population of Malaysia, 2017)

Table 3.1: Table of Section Properties

Table 3.2: Material properties from the result of tensile test (Hashim, 2013)

Table 3.3: Data of maximum nodal displacements of C-section

Table 4.1: Comparison result between C-channel steel section with openings and C-channel steel section without opening

Table 4.2: Comparison between the nonlinear analysis results of C channel section without opening and C-channel section with different edge distance for various opening spacing

Table 4.3: Comparison between yield moment and ultimate moment of C-channel without opening and C-channel with different thickness

Table 4.4: Comparison result between C-channel steel section with 0.4D of square opening with 0.3L edge opening and 0.1L opening space and C-channel steel section without opening

## LIST OF FIGURES

Figure 1.1 Increase of population in Malaysia from 1950 to 2017 (Malaysia population, 2017)

Figure 1.2: Shape of cold-formed steel sections

Figure 1.3: Section symbols in cross section of a cold-formed Lipped channel steel section. (Lian.Y et al. 2016)

Figure 1.4: Geometric configurations of web openings.

Figure 2.1: Weak areas of perforated steel section and geometrical key parameters (Tsavdaridis et al.,2012)

Figure 2.2: Virendeel mechanism and location of plastic hinge (Chung et al., 2000)

Figure 2.3 Development of the fillet corner web opening shape (Wang et al., 2014)

Figure 3.1: Triangular thin shell (TS3 and TSL6) and quadrilateral thin shell (QSI4 and QSL8) (LUSAS Modeller, 1999)

Figure 3.2 Flow chart of modelling by using LUSAS software

Figure 3.3: Create new model

Figure 3.4: Coordinate setting for origin

Figure 3.5: Coordinate table to set an origin

Figure 3.6: X, Y and Z coordinate box

Figure 3.7: Sweep box

Figure 3.9: Coordinate/ Points icon for creating a square

Figure 3.10: Icon for create holes

Figure 3.11: Surface mesh dialog box

Figure 3.12: Geometric surface

Figure 3.13: Define elastic properties

Figure 3.14: Define plastic properties

Figure 3.15: Support toolbar

Figure 3.16: Loading toolbar

Figure 3.17: Table for loading value

Figure 3.18: Section after meshing

Figure 3.19: Whole section with assigned support and loading condition

Figure 3.20: Icon for Nonlinear and Transient

Figure 3.21: Nonlinear and Transient Dialog

Figure 3.22: Element Options dialog box

Figure 3.23: Contour dialog box

Figure 3.24: Selecting node

Figure 3.25: Graph wizard setting – Time history option

Figure 3.26: Time History Graph – X Attribute

Figure 3.27: Enter the data for X Attribute

Figure 3.28: Time History Graph – Y Attribute

Figure 3.29: Enter the data for Y Attribute

Figure 3.30: Display Graph Option

Figure 3.31: Graph of resultant displacement against number of element

Figure 4.1: House framing system

Figure 4.2: Result of analysis on bending moment of house framing system

Figure 4.3: Result on Beam 223 (Most critical beam section with highest bending moment)

Figure 4.4: C-channel steel section section with opening

Figure 4.5: Load deflection curves of C-Section with and without openings

Figure 4.6: Non-perforated C channel

Figure 4.7: 0.1L (100mm) of edge distance with 0.1L (100mm) of opening spacing

Figure 4.8: 0.1L (100mm) of edge distance with 0.2L (200mm) of opening spacing

Figure 4.9: 0.1L (100mm) of edge distance with 0.4L (400mm) of opening spacing

Figure 4.10: 0.2L (200mm) of edge distance with 0.1L (100mm) of opening spacing

Figure 4.11: 0.2L (200mm) of edge distance with 0.2L (200mm) of opening spacing

Figure 4.12: 0.2L (200mm) of edge distance with 0.3L (300mm) of opening spacing

Figure 4.13: 0.3L (300mm) of edge distance with 0.1L (100mm) of opening spacing

Figure 4.14: 0.3L (300mm) of edge distance with 0.2L (200mm) of opening spacing

Figure 4.15: 0.3L (300mm) of edge distance with 0.4L (400mm) of opening spacing

Figure 4.16: 0.4L (400mm) of edge distance with 0.1L (100mm) of opening spacing

Figure 4.17: 0.4L (400mm) of edge distance with 0.2L (200mm) of opening spacing

Figure 4.18: 0.5L (500mm) of edge distance with 0.2L (200mm) of opening spacing

Figure 4.19: Load deflection of non-perforated C-channel section with various thickness

Figure 4.20: Load deflection of perforated C-channel section with various thickness

Figure 4.21: Graph of yield moment against thickness of section

Figure 4.22: Result of contour of displacement for C-channel section without opening

Figure 4.23: Result of contour of displacement for C-channel section with opening

Figure 4.24: Result of contour of displacement for C-channel Section with 0.4D of square opening



## LIST OF SYMBOLS

$P_y$	Design strength of the steel
$I_x$	Second moment of area about x axis
$I_y$	Second moment of area about y axis
$S$	Plastic modulus of the section
$Z$	Section modulus about major axis
$x$	Torsional index
$t$	Thickness of section
$D$	Depth of the section
$B$	Length of the flange
$C$	Length of the lip
$d_o$	Depth of Opening
$e$	Edge or end distance
$r_x$	Radius of gyration of x-x axis
$M_c$	Moment capacity
$M_u$	Ultimate moment
$M_y$	Yield moment
$\delta$	Deflection

P	Loading
$P_u$	Ultimate load
$P_y$	Yield load
L	Length of the section
A	Cross sectional area of section
E	Young's modulus
$\mu$	Poisson ratio

# CHAPTER ONE

## INTRODUCTION

### 1.1 Introduction

Over the past decades, constant population growth happened in Malaysia especially in states such as Penang and Kuala Lumpur. From an analysis shown in Figure 1.1 and Table 1.1, In 2000, population in Malaysia was registered with around 23 million people and density of 71 population per km<sup>2</sup>; while in 2017, population in Malaysia has increased to around 31 million people and density of 95 population per km<sup>2</sup>.

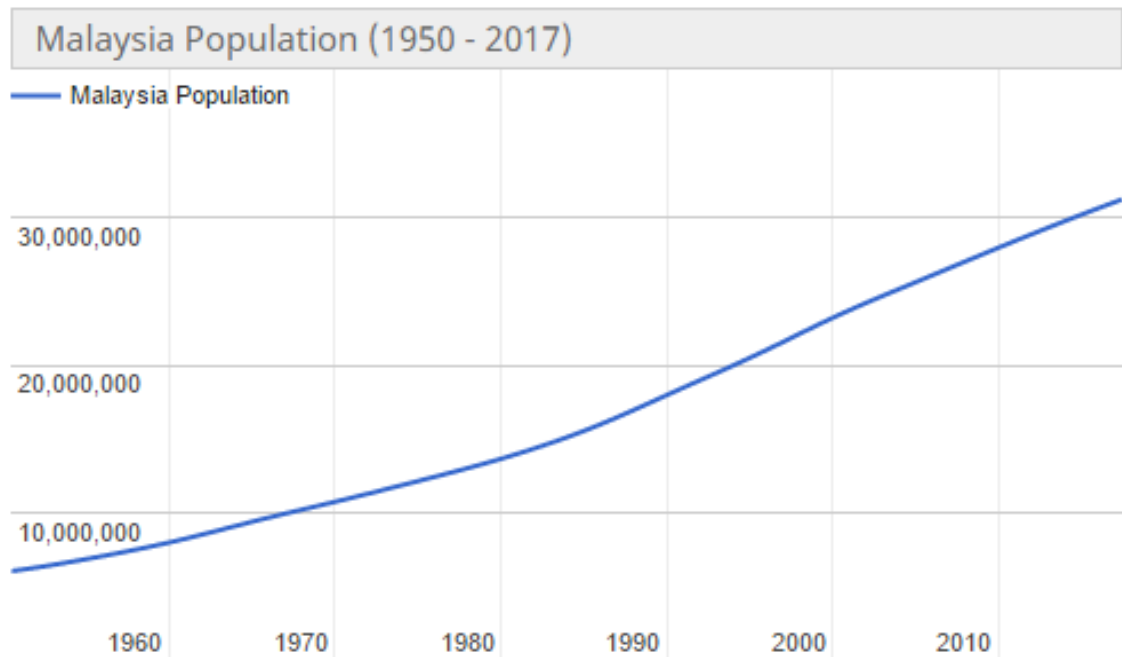


Figure 1.1 Increase of population in Malaysia from 1950 to 2017 (Malaysia population, 2017)

Table 1.1 Increase of population in Malaysia from 2000 to 2017 (Population of Malaysia, 2017)

Year	Population	Yearly % Change	Yearly Change	Density (P/Km <sup>2</sup> )
2017	31,164,177	1.34%	412,575	95
2016	30,751,602	1.39%	420,595	94
2015	30,331,007	1.53%	442,301	92
2010	28,119,500	1.74%	464,675	86
2005	25,796,124	1.95%	475,075	79
2000	23,420,751	2.48%	539,075	71

With increasing population and limited land area, there will be lack of housing area to withstand the high population. Due to inflation and unstable oil price, the rise of cost of building materials also caused the increase of average cost of house. This caused the properties especially in Penang and Kuala Lumpur are very high which may not affordable by middle income households.

Besides, Malaysia had experienced flood on December 2014 in the state of Kelantan. Therefore, house with fast construction speed is more demanding in natural disaster-prone area. Due to highly demand of housing, the usage of cold formed steel section as framing system was introduced.

## **1.2 Cold-formed steel (CFS)**

Thin-walled cold-formed steel (CFS) sections are widely used as primary and secondary framing members in housing construction, low to medium-rise office and retail buildings construction. The advantages of using cold-formed steel sections are ease of prefabrication and mass production, uniformity of quality, low weight, economy of transportation and handling, and quick and simple erection or installation. With quick installation and construction, cold-formed steel framing construction is faster and cheaper. Cost analysis in the design of open-web castellated beams has been studied by Estrada et al. (2006) and was found that the application of openings can cut down substantial materials and construction costs.

## **1.3 Characteristic of Cold-formed steel**

Cold-formed steel sections are commonly used for floor joists and other structural members. Mono-symmetric or point-symmetric open sections, such as C-sections and Z-sections as shown in Figure 1.2 are typically used in cold-formed steel joists. Discrete holes (perforations) are also commonly placed in the web of cold-formed steel beams to accommodate plumbing and electrical facilities. Figure 1.3 shows the section symbols in cross section of a cold-formed Lipped channel steel section.

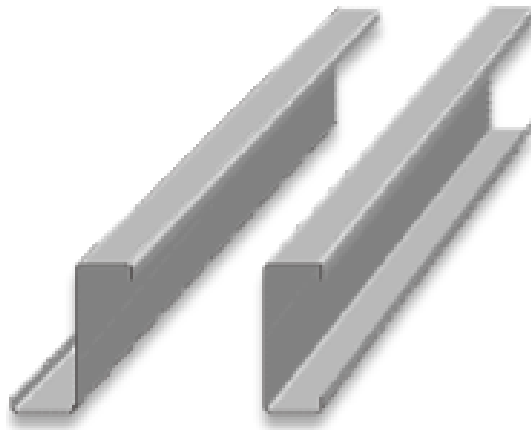


Figure 1.2: Shape of cold-formed steel sections

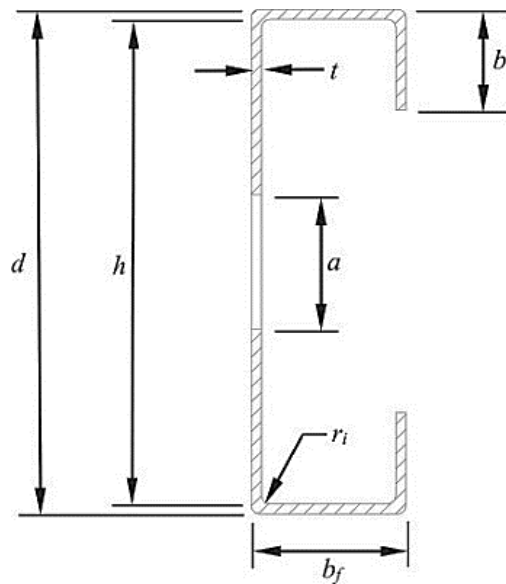


Figure 1.3: Section symbols in cross section of a cold-formed Lipped channel steel section.  
(Lian.Y et al. 2016)

### 1.3.1 Perforated Steel Section

Perforation is holes made by boring or piercing. For perforated steel section, it means that there are holes at the steel. For perforated section, the shape configuration, size of web opening and distance of opening from the support have large impact on the structural performance of the perforated section. Figure 1.4 shows some of the common geometric configurations of web openings. Tsavdaridis and D Mello, (2009) indicated that perforated section with vertical and rotated elliptical web openings have a better performance compared to circular and hexagonal web opening. This research also indicated that the reduction in the shear capacity is more pronounced when compared to the reduction in the moment capacity, as the presence of the opening in the web reduces the shear area of the section significantly whilst the reduction of the bending modulus is small.

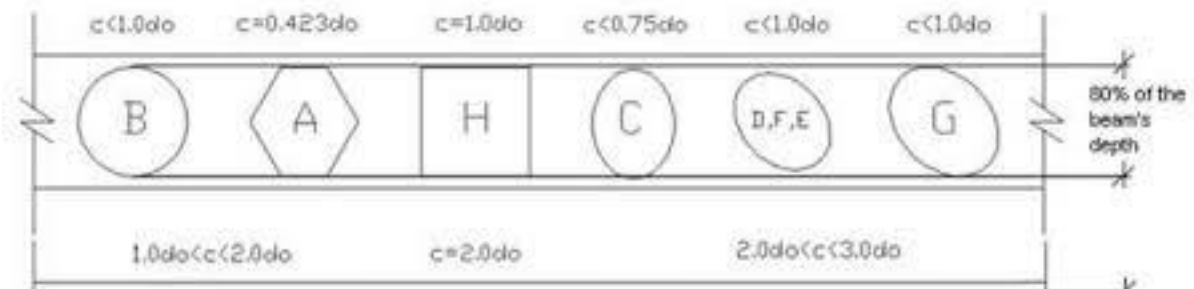


Figure 1.4: Geometric configurations of web openings. (Tsavdaridis and Mello, 2009 and 2012)

## **1.4 Problem Statement**

While the price of steel remained fluctuated throughout the years, the construction cost of cold formed steel framing homes is comparable with conventional homes built with reinforced concrete. This is due to cold formed steel framing homes are built with prefabricated cold form steel and 15% cheaper due to accuracy and speed while reinforced concrete homes normally are casted in-situ and building speed is slower compare to cold form steel framing homes. Thus, the actual construction cost of both house with cold formed steel and reinforced concrete using same framing systems will be compared.

Besides, perforation in steel beams will reduce the raw material required. Therefore, the cost of cold formed steel framing system can also be further reduced by making openings at the web surface of steel beam to produce perforated steel section.

## **1.5 Objectives**

1. To study the bending behaviour of cold form steel framing system.
2. To compare the effective cost reduction between perforated and non-perforated steel section in steel framing system.



## **1.6 Scope of work**

This research is carried out to investigate the structural behaviour related to the bending behaviour of cold formed steel structural member with perforated section in a single-story house framing system. The performance of cold formed steel structural member with perforated section will be compared with cold formed steel structural member without perforated section. Thus, the scope of work can be divided into several important parts:

- a) Determination of the model sizes, shapes, and symmetry of cold formed steel structural member with and without perforation shapes.
- b) By using Staad.Pro, the whole framing system is analysed and the most critical beam with highest bending moment is determined.
- c) By using LUSAS software, the most critical beam is analysed with different models of edge distance, spacing of opening and web thickness under bending condition to observe the bending behaviour of the beam.

## CHAPTER 2

### LITERATURE REVIEW

#### 2.1 Perforated steel section

In construction field, perforated steel plates are used regularly due to cost reduction, ease of fabrication, high strength to weight ratio and suitability for a wide range application. Researchers such as Seo and Mahendran, (2012) and Chung et al., (2001) tried to examine numerically the shapes of opening and identify the best structural behavior of the opening under the certain type of loading. These researches were aimed to provide the maximum possible web opening area without affecting the structural behavior and kept the minimum possible self-weight.

Perforation geometry mainly found in the literature are hexagonal (in some cases within extra mid-depth plate which then creates an octagonal shape), circular, rectangular, square or elongated (i.e. 'extended') and large or small perforation.

Experimental and finite element studies on perforated web beams have reported six main different modes of failure. These modes are associated with beam geometry, shape parameters, web slenderness, type of loading and provision of lateral support. These modes are vierendeel mechanism, flexural mechanism, lateral torsional buckling (LTB), rupture welded joints, web-post buckling in shear and compression buckling (Redwood, 1973; Redwood, 1969; Bower, 1968).

The presence of local bending and shear strength of the web-posts, top and bottom tee section restricted the load carrying capacity of a perforated beam (Tsavdaridis et al., 2012).

Figure 2.1 shows the weak areas of perforated steel section.

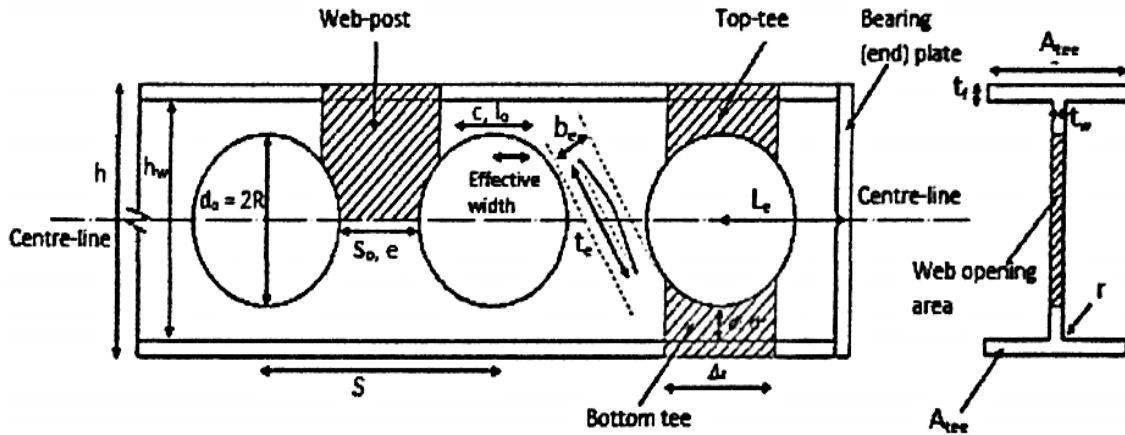


Figure 2.1: Weak areas of perforated steel section and geometrical key parameters (Tsavdaridis et al.,2012)

The failure focused for perforated steel section is vierendeel failure. Vierendeel mechanism is one of the failures that is associated with high shear force acting on the beam. It is the most dominant failure mode of perforated beams with isolated large web openings (Tsavdaridis et al., 2012). Plastic hinges are formed at the corner of the web opening shapes or at the specific positions deform tee section above the web opening to a stretched shape (Tsavdaridis et al., 2013). The transfer of vertical shear force across the web opening can cause local bending moment, termed as the vierendeel bending moment which is the root cause of vierendeel failure. Vierendeel mechanism occurs when the continuous formation of plastic hinges at the ends of four tee sections above and below the opening under the combination of the vierendeel bending moment, local axial force, and local shear force (Seo and Mahendran, 2012)

Experimental results of Redwood and McCutcheon (1998) were used by Tsavdaridis and Mello (2012) to validate the FE model on the vierendeel bending study of perforated steel beams with various novel web opening shapes. The global shear capacities were reduced when the load distribution across the web openings occurred and formation of the vierendeel mechanism was acting on the top and bottom tee sections. Perforated sections with non-standard vertical and inclined elliptical web openings behave more effectively compared to standard circular and hexagonal web openings, mainly in term of stress distribution. They can conclude that the position and shapes of the web opening have affected the structural behavior of the perforated beam.

Chung et al. (2000) investigated the failure modes in steel beams with circular web openings. At the top tee sections on the lower moment side of the web opening, the load capacity of the beams was assumed to be limited by the formation of plastic hinges. The beams could carry an additional load until four plastic hinges at critical locations of the perforated sections (as shown in Figure 2.2) were developed to form a vierendeel mechanism. A linear interaction formula was used to assess the moment capacity of the tee section above and below the web openings under co-existing axial and shear force. The method was regarded as conservative since the formation of plastic hinges at the top tee sections on the lower moment side examined in detail with the plastic hinges formed on the lower moment side (LMS) and the high moment side (HMS) of the web openings separately.

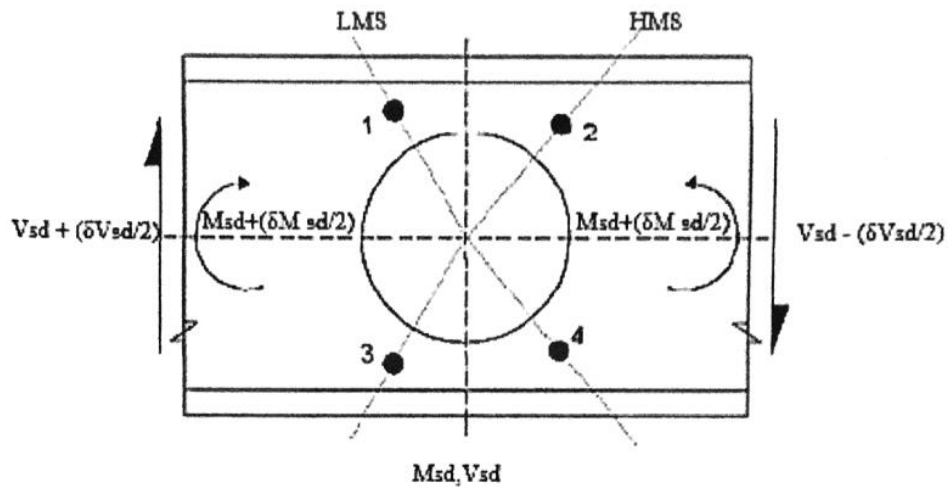


Figure 2.2: Vierendeel mechanism and location of plastic hinge (Chung et al., 2000)

Besides, Wang et al. (2014) used the validated FEM to investigate on vierendeel mechanism failure and examine the effects on the fillet corner web opening dimension on the load bearing capacity of the Castellated Steel beam (CSBs) as shown in Figure 2.3. The studies of the opening shapes include the newly-developed fillet corner opening, circular, hexagonal, rectangular, and sinusoidal opening and the results obtained were compared. The load bearing capacity of CSBs are affected by the parametric study such as fillet radius, expansion ration (the height of the castellated beam to that of the original steel beam), opening length and shapes of the web opening, the fillet radius can promote the stress distributions around the web opening, which can increase the load bearing capacity of the web-perforated members. The fillet radius which equals to a quarter of the opening height was the best choice for the proposed fillet corner web opening shapes. The global bending moment capacity of the perforated member increases as the expansion ratio increases. However, the vertical shear resistance decreases significantly because there is only a small solid web left for the resistance of the vertical shear force. With the increase

in the opening length, the vertical shear capacity of the perforated member decreased due to the increase in the local vierendeel moment.

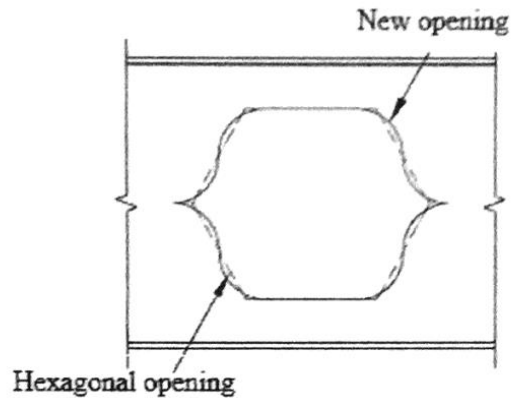


Figure 2.3 Development of the fillet corner web opening shape (Wang et al., 2014)

Soltani et al. (2012) proposed a finite element model to evaluate the resistance of castellated beams with the hexagonal and octagonal opening. Typical local failures of castellated beams consist of vierendeel mechanism, yielding or buckling of the web-post in shear or in compression and fracture of the welded joint. These failures were related to the geometry of the upper and bottom tee sections and the web-posts that bound the openings. For webs with large opening lengths under high shear to moment ratio, vierendeel mechanism was susceptible to occur. The vierendeel moment or secondary moment was due to the transfer of shearing forces across the opening. For castellated beams with openings, the plastic hinges were formed at the corners of the critical openings. Liu and Chung (2001) proposed an empirical shear moment interaction curve at the perforated sections to prevent the vierendeel mechanism on steel beams with large web

opening. It was used for practical design of steel beams with medium to large circular web openings against the vierendeel mechanism.

## **2.2 Bending resistance and ultimate strength**

Bending resistance of the perforated section should be sufficient to resist the applied bending moment. Zhou et al. (2012) investigated the elastic deflections of simply supported steel I-beams containing large rectangular web opening by using the displacement method and finite elements analysis. From the comparison of both methods, they calculated that the secondary bending moments without solving redundant forces. It can be solved by assuming the point of contra-flexure at the middle point of the upper and lower beam. Secondary bending moments have a great effect on the deflections, particularly in the region of the opening. In contrast, the effect of the primary bending moment was small and it was neglected.

The different shape of web opening such as circular, hexagon, octagon and square of steel beam was analyzed by Siddh and Pachpor (2011). Finite element analysis (ANSYS software) was analyzed for constant loading, different area of the opening and support condition. The deflection pattern at the center of the beam was observed by changing the beam's section and position of openings along the length of the beam. The deflection in the solid web beams was less as compared to the beam with openings.

Yatim et al. (2013) examined the effects of opening size and degree of shear connection to assess their influence on the shear strength and behavior of the girders in the case of the composite plate girders containing square of circular web openings. It was observed that the ultimate load capacity drops significantly with the opening size and shear connectors

spacing. In addition, the rate of reduction is dependent upon the span length and slenderness of the girders. As for the prediction of load-deflection behavior, the comparisons with the curves obtained from LUSAS agree well in most cases. It started from the initial stages of loading to the respective yield point, thus confirming the accuracy of the present method.

### **2.3 C-channel cold formed steel under bending**

Ling (2015) conducted 63 set of nonlinear analysis to investigate the bending behaviour of C-channel Section with different shapes such as circular, square, diagonal and hexagonal openings and with various sizes such as 0.3D, 0.4D, 0.5D, 0.6D and 0.7D, where D is the depth is the depth of the section. The results showed that C-channel Section with 0.4D of square opening give highest yield moment compared to other opening shapes.

### **2.4 Summary**

In summary, many studies have been done on cold-formed steel, C-section and section with perforations, and were reviewed in this chapter. There are a few researches are carried out to find out the failure modes such as vierendeel mechanism, flexural mechanism, lateral torsional buckling (LTB), rupture welded joints, web-post buckling in shear and compression buckling openings. Lastly, the use of open-web beams can save material and construction costs. However, the researches on C-channel steel are still insufficient. There is no research study about bending behaviour of C-channel section with perforations for house framing system. Further studies are required to establish the performance of C-channel steel with openings for house framing system.



## CHAPTER 3

### METHODOLOGY

#### 3.1 Introduction

This chapter describes the method used to develop a finite element model in order to study the bending behaviour of cold formed steel structural member with perforated section in house framing system. Cold formed steel structural member without opening will be used as a control specimen.

#### 3.2 Numerical Study on Bending of C-channel Steel Section

Finite element software LUSAS was used to determine the bending behaviour of both sections in this study. The yield load was obtained through nonlinear load deflection graph. The table of section properties for the section used is provided in Table 3.1.

D	152mm	$I_x$	2.42E6mm <sup>4</sup>		
B	51mm	$I_y$	0.1797E6mm <sup>4</sup>		
R	22mm	Centroid, c	12.02mm		
t	3.0mm	$Z_x$	31.9E3mm <sup>3</sup>		
Section Area (mm <sup>2</sup> )	735	$Z_y$	4.47E3mm <sup>3</sup>		
Mass per unit length	Galv. (kg/m)	5.86	$r_x$		57.4mm
	Black (kg/m)	5.77	$r_y$		15.64mm

Table 3.1: Table of Section Properties

### 3.2.1 Perforation Shapes and Sizes

C-Channel Section with 0.4D of square opening referred to the research from (Ling,2015) will be a constant throughout the whole research.

### 3.2.2 Material Properties

Material assigned to the model is referred to the research from Hashim, (2013) as in Table 3.2. The Poisson ratio used in this study is 0.3 for all the models. In this study, deformation is only considered in the elastic zone of the materials.

Table 3.2: Material properties from the result of tensile test (Hashim, 2013)

Young's modulus, E	226.53 GPa
Poisson's ratio	0.3
Yield Stress	387 N/mm <sup>2</sup>
Hardening Gradient	5.664kN/mm <sup>2</sup>
Plastic Strain	0.481

### 3.2.3 Thickness of Section

In this study, thickness of section,  $t = 1.0$  mm, 1.5mm, 2.0 mm, 2.5 mm, and 3.0 mm was investigated.

### 3.2.4 Model Meshing

In order to obtain a more accurate solution element aspect ratio, element mesh and the convergence result had to be considered. Shell elements were used to model 3 dimensional structures whose behaviour is dependent upon both flexural and membrane effects. LUSAS incorporates both flat and curved shell elements, which may be either triangular or quadrilateral. Both thin and thick shell elements were available (LUSAS Modeller, 1999).

Thin shell element was chosen to represent the element type, element shape as the quadrilateral (QLS8) and interpolation order in quadratic. In LUSAS, there are four type of thin shell elements. For instance, triangular thin shell (TS3 and TSL6) and quadrilateral thin shell (QSI4 and QSL8) as shown in Figure 3.1. Element size is determined from the convergence study which will be discussed in Section 3.4.

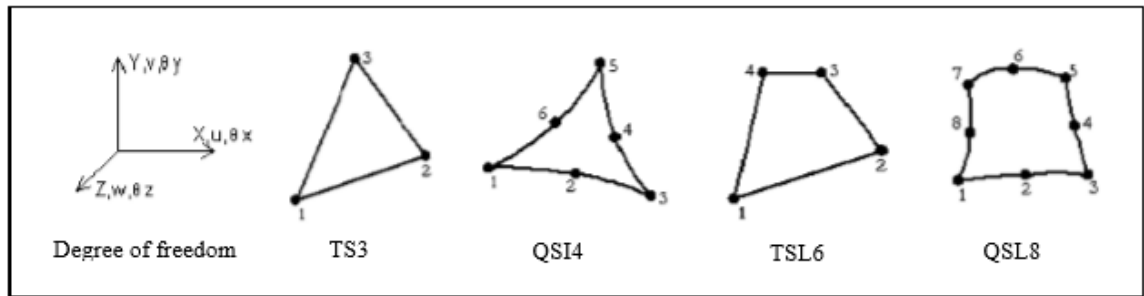


Figure 3.1: Triangular thin shell (TS3 and TSL6) and quadrilateral thin shell (QSI4 and QSL8) (LUSAS Modeller, 1999)

### 3.3 Finite Element Analysis LUSAS

In this study, LUSAS finite element software is used to carry out nonlinear analysis.

Figure 3.2 shows the summary of general steps in LUSAS.

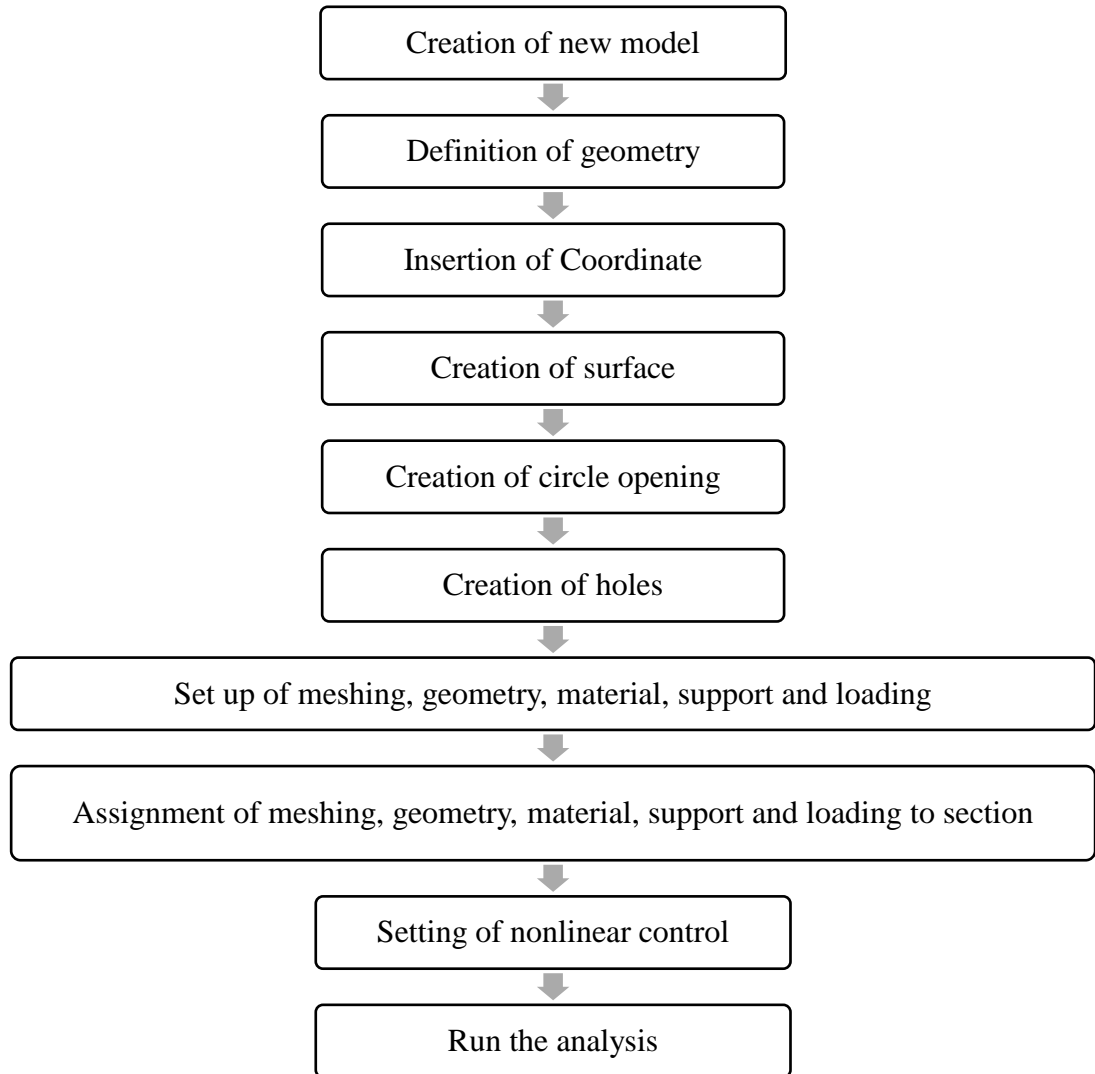


Figure 3.2 Flow chart of modelling by using LUSAS software

### 3.3.1 LUSAS Procedure in Modelling Process

The detailed procedures in developing nonlinear finite element model with openings are described in this section, as shown from Figure 3.3 to Figure 3.30.

#### 1. Create new model

- File>new
- Enter the file name as C-Section Steel with Opening
- Enter the title as C-Section with Opening
- Set the units as KN, mm, kt, s, C
- Set the vertical axis option as Y
- Proceed with the OK button

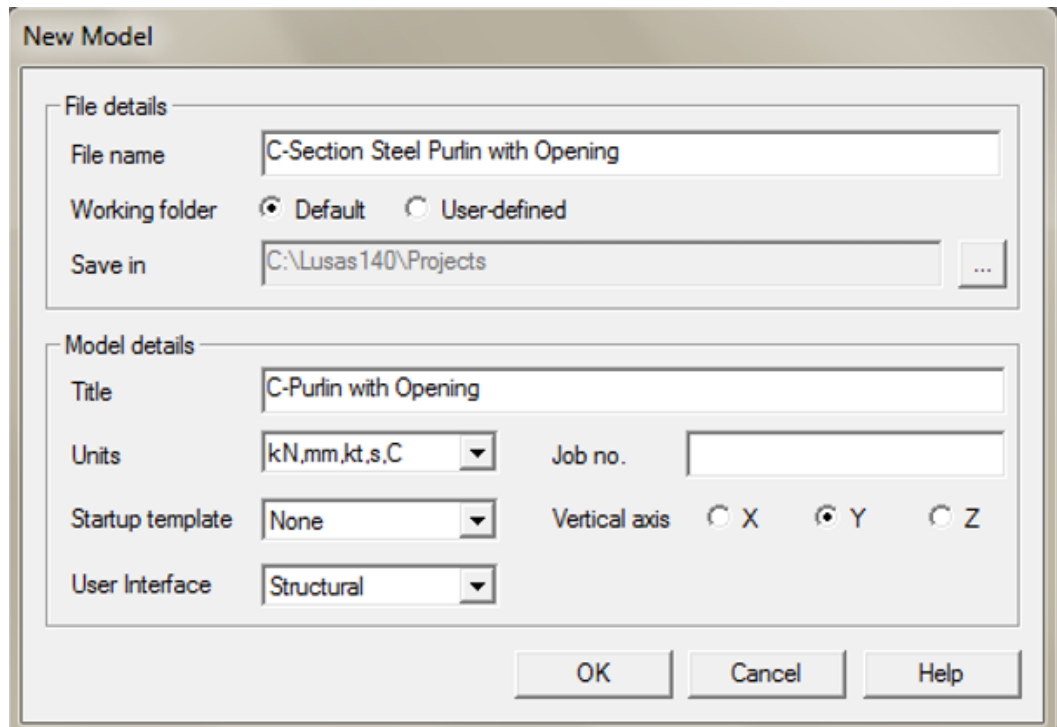


Figure 3.3: Create new model

## 2. Define geometry

- Geometry>Point>Coordinates
- Enter coordinates (0,0,0) to set as the origin
- Click OK button

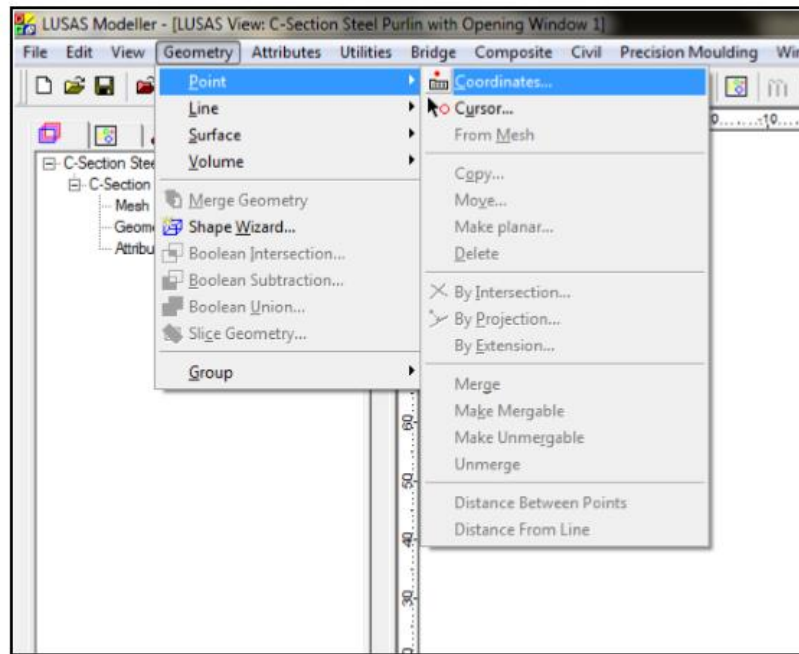


Figure 3.4: Coordinate setting for origin

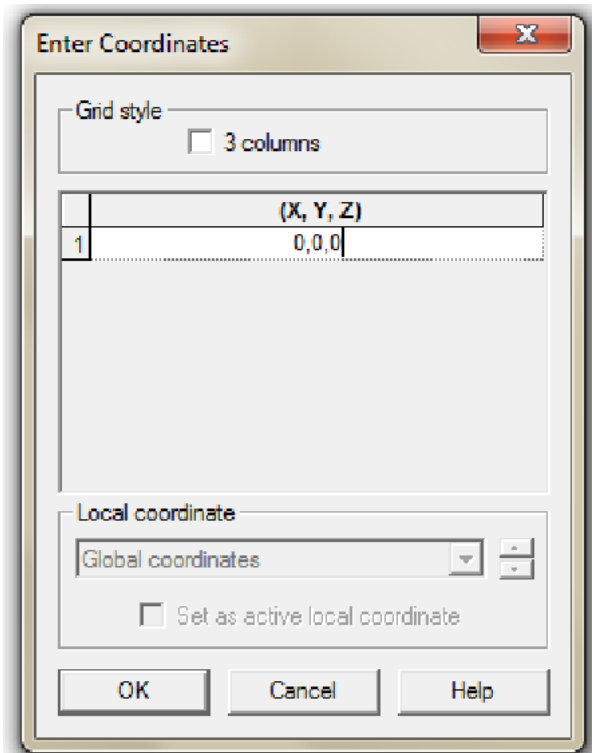


Figure 3.5: Coordinate table to set an origin

### 3. Copy and create surface from the origin point

- Highlight the origin point
- Right click and click copy
- Enter the length for x-axis
- Repeat it for y-axis and z-axis
- Joint the point with surface

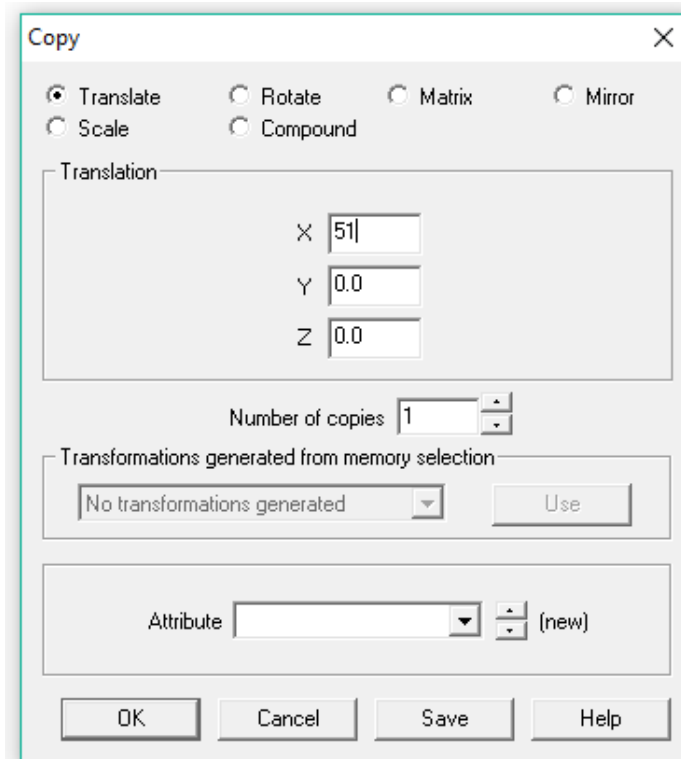


Figure 3.6: X, Y and Z coordinate box

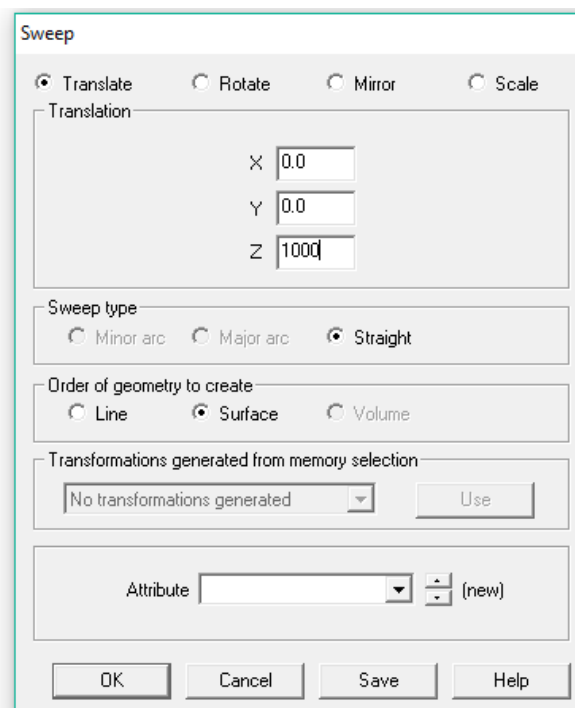


Figure 3.7: Sweep box



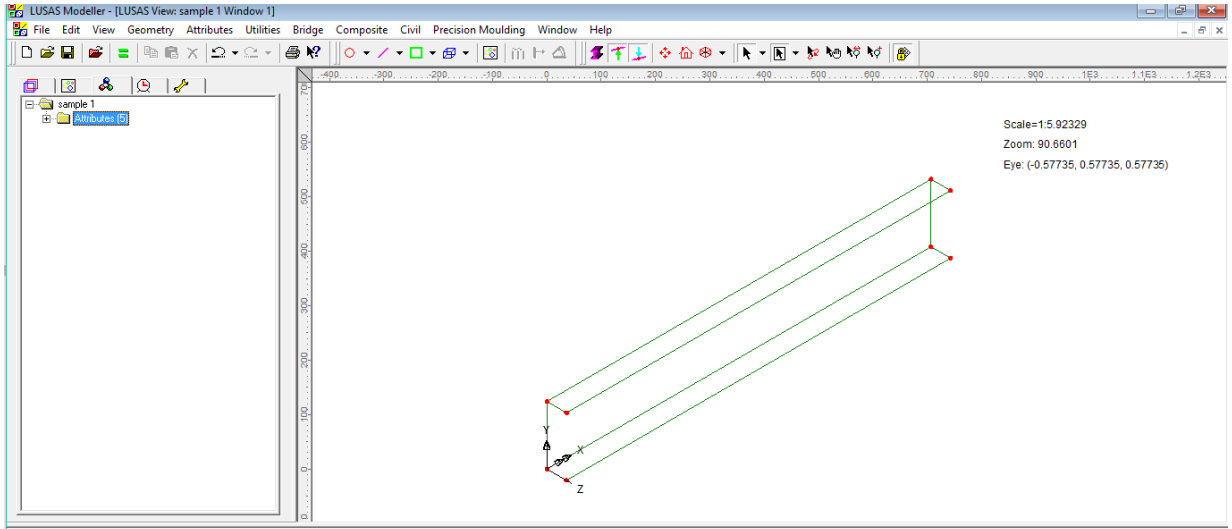


Figure 3.8: C-section after creating the surface

#### 4. Create opening

- Enter the points/coordinates for the square
- Copy the number of square

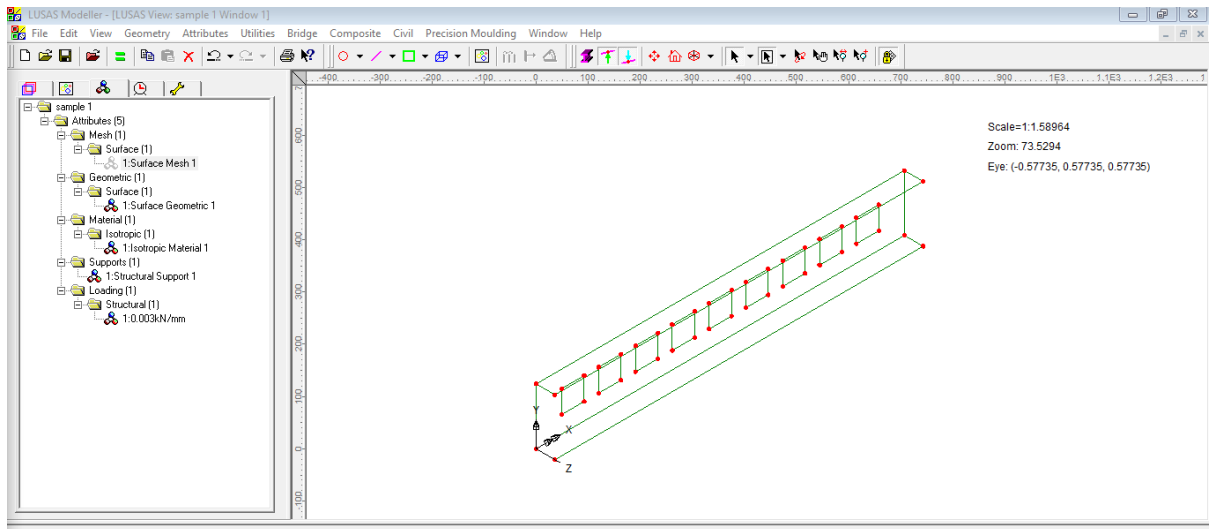


Figure 3.9: Coordinate/ Points icon for creating a square

## 5. Creates holes

- Highlight whole section
- Geometry>Surface>Holes>Create
- Click OK with '*Delete geometry defining holes*'

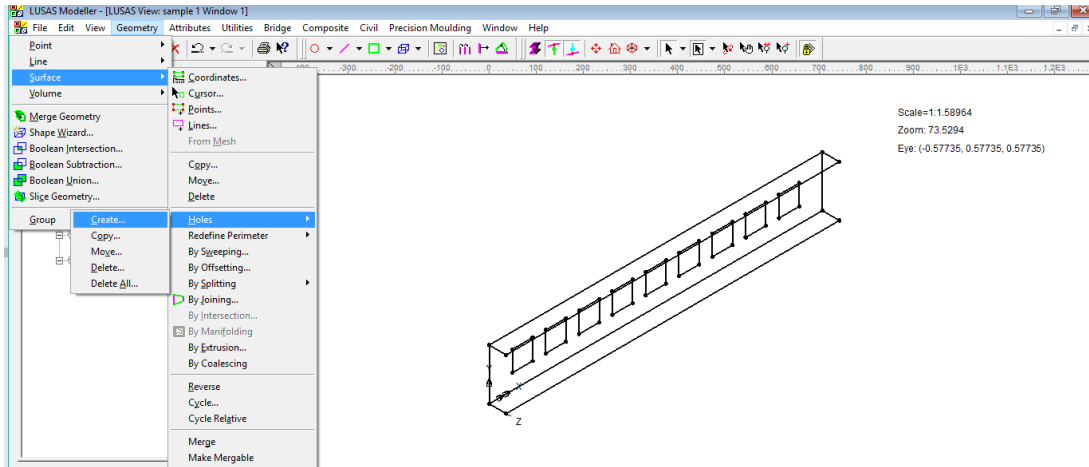


Figure 3.10: Icon for create holes

## 6. Mesh

- Attribute>Mesh>Surface
- Suitable element size is determined from convergence study which is described later in Section 3.4.